Nonrepeatable Run-out Rejection Using Online Iterative Control for High-Density Data Storage

Chee Khiang Pang[1,2], Wai Ee Wong[1], Guoxiao Guo[1], Ben M. Chen[2], *Fellow, IEEE*, and Tong Heng Lee[2]

[1]A*STAR Data Storage Institute, National University of Singapore, 117608 Singapore
[2]Department of Electrical and Computer Engineering, National University of Singapore, 117576 Singapore

The spectra of disturbances and noises affecting precise servo positioning for ultrahigh-density storage in future hard disk drives are time-varying and remain unknown. In this paper, we propose an online iterative control algorithm that sets the measured position error signal (PES) into the servo system to achieve high track densities by minimizing the square of the $\mathcal{H}_2$-norm of the transfer function from nonrepeatable run-out (NRRO) disturbances to the true PES. It is not necessary to solve any algebraic Riccati equations and linear matrix inequalities. The algorithm constructs an online repeatable run-out estimator to extract NRRO components for gradient estimates, thereby preventing the controller parameters from being trapped in a local minima. Experimental results on a PC-based servo system for a spinstand show an improvement of 22% in 3σ NRRO and suppression of baseline NRRO spectrum.

Index Terms—**Hard disk drives, iterative control, NRRO, PES, self servotrack writing (SSW), servo track writing (STW).**

I. Introduction

In the hard disk drive (HDD) industry, the areal density is continuously growing and targeting to achieve more than 1 Tb/in^2 through use of perpendicular recording technologies. In turn, this demand for higher track density directly translates to a read/write (R/W) head position accuracy of more than 400 kilotracks per inch (kTPI). However, many contributing factors exist and limit the achievable track density. One of the major contributors is the NRRO generated from the disk media and spindle vibration, which is induced by the windage noise within the disk stack mounted on the rotating spindle motor.

Many considerable efforts have been made to design servo control systems to reduce the effect of actuators' vibrations in operation of HDDs, especially on the NRRO error induced by the disk-spindle system, disk fluttering, and head media defects. As with all HDD designs, the efficiency of controlling vibrations and structural noise depends on the dynamic behavior of the overall system considering parametric variations among HDDs in terms of resonant frequencies, length, mass, force (or torque) constant, R/W element, etc. System designers are continually challenged to bring all of these elements together to produce the "optimal" design that meets the criteria for the various applications the HDDs are designed for. As such, self-optimizing servo controller designs are hence essential for the millions of HDDs produced by the HDD industries per day.

Several robust and optimal controller design methods using μ-synthesis via D-K iteration [8], as well as $\mathcal{H}_2/\mathcal{H}_\infty$ designs with algebraic Riccati equations (AREs) and linear matrix inequalities (LMIs) [5], [11] have been proposed. However, because of the small damping ratios and high natural frequencies of the actuators involved, numerical instabilities during controller synthesis often arise due to ill-conditioned system matrices, prompting servo designers to doubt the integrity of the solutions.

As such, iterative learning control (ILC) or repetitive control (RC) techniques have also been introduced into the HDD industry. In [7] and [14], the authors used performance index-based rule to tune track-following controller and repetitive controller for minimum track mis-registration (TMR). The authors in [9] reinject measured PES into the servo system for precise repeatable run-out (RRO) estimation. Incidentally, reinjection of collected information back into the servo system for gradient estimates had been reported in the iterative feedback tuning (IFT) technique by authors in [6].

In this paper, an online iterative control algorithm (OICA) is proposed to tune the controller parameters to minimize the square of the $\mathcal{H}_2$-norm from disturbances and noise spectra of unknown spectra to true PES for more effective NRRO rejection. The NRRO information is extracted from the difference between measured PES and estimated RRO using an online RRO estimator. The parametric gradients required for OICA are computed by reinjecting the NRRO into closed-loop system—similar to that suggested in [6] and without having to solve any AREs and LMIs. The proposed OICA is a special class of explicit online optimization with fixed controller structures [19] based on the $\mathcal{H}_2$ control criterion, and can be readily applied to the STW and SSW processes in HDD industries to prevent error propagation issues [18].

The rest of the paper is organized as follows. Section II describes the control problem formulation when minimizing the the square of the $\mathcal{H}_2$-norm of transfer function from disturbance and noise sources to true PES. Section III details the components in the proposed OICA and the procedures in obtaining the essential gradient estimates for parametric updating using NRRO.

Digital Object Identifier 10.1109/TMAG.2006.890242

Color versions of one or more of the figures in this paper are available online at http://ieeexplore.ieee.org.

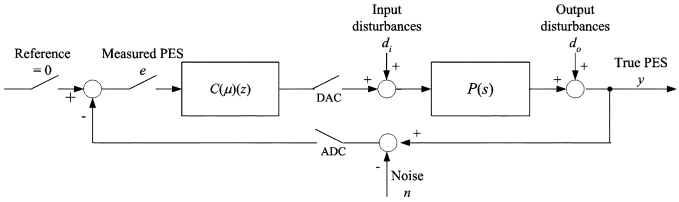

Fig. 1. Block diagram of a typical HDD servo system with input disturbances d_i, output disturbances d_o, and noise n contaminating true PES y.

The performance of the proposed OICA is verified with simulation and experimental studies using a PC-based servo system on a spinstand [15] in Section IV. Our conclusion and future work directions are summarized in Section V.

II. Control Problem Formulation

The block diagram of a typical sampled-data HDD servo system is shown in Fig. 1. From Fig. 1, the true PES y can be derived by the following relation:

$$\begin{aligned} y &= \frac{P}{1+C(\mu)P}d_i + \frac{1}{1+C(\mu)P}d_o \\ &\quad + \frac{C(\mu)P}{1+C(\mu)P}n \\ &= S(\mu)Pd_i + S(\mu)d_o + T(\mu)n \end{aligned} \tag{1}$$

where μ is a vector of controller parameters and P is the plant to be controlled. $C(\mu)$, $S(\mu)$, and $T(\mu)$ denote the feedback controller, sensitivity transfer function, and complementary sensitivity transfer function of the stable closed-loop servo system parameterized by μ, respectively. d_i, d_o, and n are the input disturbances, output disturbances, and noise sources contaminating true PES y, respectively. For high TPI in future HDDs, the TMR budget will have to be minimized when the HDD servo system is subjected to input disturbances d_i, output disturbances d_o, and noise sources n, packed as a vector w.

Let the transfer function of the disturbance sources w to true PES y be defined as T_{yw}. When the number of collected PES samples N are large enough in HDDs, the limit of the $\mathcal{H}_2$-norm of T_{yw} can be expressed as [11]

$$||T_{yw}||_2 = \sqrt{\frac{1}{N-1}\sum_{k=1}^{N} y^2(k)} \tag{2}$$

assuming that the sampled variance is an unbiased estimate of the unknown true PES variance. As such, the following quadratic cost function $J(\mu)$ is proposed to minimize the square of $\mathcal{H}_2$ norm in (2) parameterized by μ as

$$\begin{aligned} J(\mu) &= ||T_{yw}||_2^2 \\ &= \frac{1}{N-1}\sum_{k=1}^{N} y^2(k). \end{aligned} \tag{3}$$

While measured PES e remains as the only accessible quantity in HDDs, minimizing the square of TMR of true PES y is done via minimizing the square of TMR of measured PES e, i.e., the controller minimizing the measured PES e also minimizes the true PES y. The proof of this argument is found in the appendix of [7] and is omitted here for brevity but without loss of generality. It should be noted that the measured PES e consists of RRO and NRRO components.

As such, the optimal controller parameter μ^* is thus defined as

$$\mu^* = \min_{\mu\in\Sigma} J(\mu) \tag{4}$$

where Σ is the set of all stabilizing controllers. By finding the partial derivative of $J(\mu)$ with respect to μ

$$\frac{\partial J}{\partial \mu} = \frac{2}{N-1}\sum_{k=1}^{N} y(k)\frac{\partial y}{\partial \mu}(k) \tag{5}$$

and setting (5) to zero, we can obtain the minima (local or global) μ^* directly. While it is not mathematically tractable to find a direct solution to (5) with the main obstacle being evaluation of partial derivative of true PES y with respect to controller parameter vector $(\partial y/\partial \mu)(k)$, taking partial derivative of (1) with respect to control parameter μ yields

$$\begin{aligned} \frac{\partial y}{\partial \mu} &= -\frac{P^2}{[1+C(\mu)P]^2}\frac{\partial C}{\partial \mu}d_i - \frac{P}{[1+C(\mu)P]^2}\frac{\partial C}{\partial \mu}d_o \cdots \\ &\quad - \frac{C(\mu)P^2}{[1+C(\mu)P]^2}\frac{\partial C}{\partial \mu}n + \frac{P}{1+C(\mu)P}\frac{\partial C}{\partial \mu}n \\ &= -S(\mu)^2P^2\frac{\partial C}{\partial \mu}d_i - S(\mu)^2P\frac{\partial C}{\partial \mu}d_o \cdots \\ &\quad - C(\mu)S(\mu)^2P^2\frac{\partial C}{\partial \mu}n + S(\mu)P\frac{\partial C}{\partial \mu}n \\ &= -S(\mu)P\frac{\partial C}{\partial \mu}[S(\mu)Pd_i + S(\mu)d_o \cdots \\ &\quad + C(\mu)S(\mu)Pn - n] \\ &= -S(\mu)P\frac{\partial C}{\partial \mu}[S(\mu)Pd_i + S(\mu)d_o + T(\mu)n - n]. \end{aligned} \tag{6}$$

Substituting (1) into (6), the partial derivative $(\partial y/\partial \mu)$ can also be expressed as

$$\frac{\partial y}{\partial \mu} = -S(\mu)P\frac{\partial C}{\partial \mu}[y-n] \tag{7}$$

which implies the required numerical gradient estimate of $(\partial y/\partial \mu)$ can be obtained by filtering $(y-n)$ with partial derivative of controller with respect to controller parameter vector $(\partial C/\partial \mu)(\mu)$, and shock transfer function $S(\mu)P$.

Using the proposed scheme, $(\partial y/\partial \mu)$ is not affected by input disturbances d_i and output disturbances d_o as can be seen from (7) and only measurement noise n permeates through to the gradient estimate $(\partial y/\partial \mu)$. However, if we assume that the noise n is of zero mean, then the effects of n on the gradient estimate of cost function $(\partial J/\partial \mu)$ will be negligible if N is large due to the expectation (or averaging) operation from (5). As such, (7) can also be approximated and rewritten as

$$\frac{\partial y}{\partial \mu} \approx -S(\mu)P\frac{\partial C}{\partial \mu}e \tag{8}$$

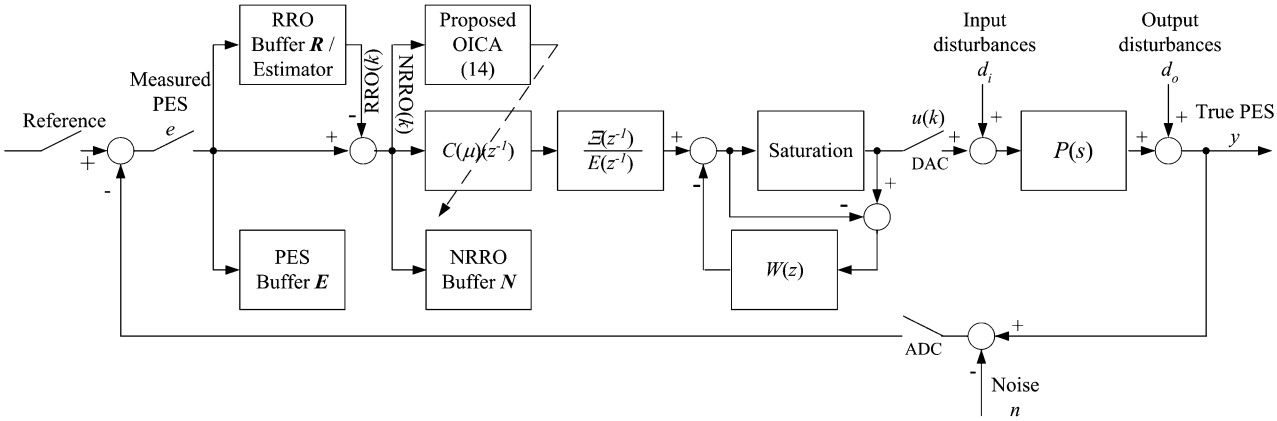

Fig. 2. Block diagram of spinstand experiment setup with RRO estimator, anti-windup compensator $W(z)$, and actuator saturation considerations.

with zero reference during track-following control. The gradient estimate of cost function $(\partial J/\partial \mu)$ will hence be a sufficiently accurate unbiased estimate and will be used in future sections for the proposed OICA using NRRO.

Remark 1: If $C(\mu)$ is a finite impulse response (FIR) filter of the form

$$\begin{aligned} C(\mu)(z^{-1}) &= \mu_0 + \mu_1 z^{-1} + \cdots + \mu_n z^{-n} \\ &= \boldsymbol{\mu}^T \boldsymbol{\xi}(z^{-1}) \end{aligned} \tag{9}$$

where $\boldsymbol{\mu} = [\mu_0\, \mu_1 \cdots \mu_n]^T$ and $\boldsymbol{\xi} = [z^0\, z^{-1} \cdots z^{-n}]^T$, then the partial derivative of controller with respect to controller parameter vector $(\partial C/\partial \mu)$ is given by

$$\frac{\partial C}{\partial \mu} = \boldsymbol{\xi}(z^{-1}) \tag{10}$$

or a vector of delay operators.

Remark 2: From (7), it can be seen that we can use an online approach by injecting the result as input disturbance d_i to be filtered by shock transfer function $S(\mu)P$ and then filtering the new measured PES e offline with $(\partial C/\partial \mu)$ to obtain the required gradient estimate $(\partial y/\partial \mu)$ required for computing the gradient of cost function $(\partial J/\partial \mu)$ using (5). However, due to control signal saturation (leading to closed-loop instability) of actuators used for nanopositioning in storage systems when signals are injected as input disturbance d_i, this method of injecting measured PES e as input disturbance d_i is not used in this paper.

Remark 3: Alternatively, we can set measured PES e as reference into the servo system—which in essence is equivalent to filtering by sensitivity transfer function $S(\mu)$, and then post-filtering the new measured PES offline with $(\partial C/\partial \mu)$ and mathematical model of plant P to obtain $(\partial y/\partial \mu)$ required for computing the gradient of cost function $(\partial J/\partial \mu)$ with (5). This method (though less satisfactory as we rely on the accuracy of the mathematical model of plant P) will be used and explored in future sections of this paper.

III. Online Iterative Control Algorithm

Assuming that the initial conditions of the plant and the controllers are the same in all experiments and the experiment interval N is sufficiently large when compared to the time constants of the closed-loop system for stationarity, the components of the proposed OICA and methodologies to determine the gradient estimate of $(\partial y/\partial \mu)$ using NRRO with and without an extraneous sensor using an iterative approach are detailed in this section.

A. RRO Estimator

Before we use NRRO for estimating the gradient of $(\partial y/\partial \mu)$, an online RRO estimator is constructed to extract NRRO components from measured PES e. It should be noted that the NRRO components are assumed to be of zero mean.

As most of the RRO components enter the servo loop as output disturbances d_o (which is valid as most of the RRO components arise from disk-spindle rotation), the RRO estimator is constructed and stored in RRO buffer $\boldsymbol{R}$ as shown in Fig. 2 by ensemble averaging the logged measured PES e data in PES buffer $\boldsymbol{E}$ and dividing by sensitivity transfer function $S(\mu)$ at each iteration i offline. The NRRO components can then be obtained by the difference between measured PES e from PES buffer $\boldsymbol{E}$ and output of RRO buffer $\boldsymbol{R}$. To prevent the OICA from being "trapped" in a local optimum due to insufficient persistent excitation, the RRO components are not used for gradient estimations of $(\partial y/\partial \mu)$. After RRO compensation, the servo problem can be reformulated into a disturbance rejection problem with NRRO as output disturbance sources. Any nonlinear media and head effects are considered as initial conditions of the disturbance rejection problem with unknown disturbance frequency spectrum. The NRRO components will be used as reference for the gradient estimation of $(\partial y/\partial \mu)$ as shown in Fig. 2.

B. Gradient Estimation Using NRRO Without Extraneous Sensor

First, the measured PES e in PES buffer $\boldsymbol{E}$ from previous iteration $i-1$ is set as reference into the closed-loop servo system as suggested in Remark 3 with RRO compensation as shown in Fig. 2. The resultant data now consists of NRRO components and is used to obtain the gradient $(\partial y/\partial \mu)$ using (8). As such, the experimental gradient estimate $(\widehat{\partial y/\partial \mu})$ using NRRO components can be obtained from (8) by post-filtering with $(\partial C/\partial \mu)$ and plant model P as suggested earlier in Remark 3 of Section II. As such, we can expect more parametric adjustments and at natural frequencies of plant's resonant

modes and frequencies positive sensitivity from the shock transfer function $S(\mu)P$.

Using these data and the previously stored NRRO data in buffer $\boldsymbol{N}$, (5) is used to calculate the partial derivative of cost function with respect to controller parameter $(\partial J/\partial\mu)$ at current iteration i. This gradient will be essential for controller parameter update which will be detailed in future subsections.

C. Gradient Estimation Using NRRO With Extraneous Sensor

With additional sensors—e.g., using the PZT elements as actuator and displacement sensor simultaneously with self-sensing actuation (SSA) [12], the experimental gradient estimate $(\partial y/\partial\mu)$ using NRRO components derived earlier can be improved.

Assume that the extraneous sensor introduces a measurement noise source n_s. As such, the measured true PES y_s from the extraneous sensor is given by

$$y_s = y + n_s \tag{11}$$

and the gradient $(\partial y/\partial\mu)$ in (7) using NRRO components after RRO compensation with the proposed RRO estimator is given by

$$\frac{\partial y}{\partial \mu} = -S(\mu)P\frac{\partial C}{\partial \mu}[y_s - n - n_s]. \tag{12}$$

Similarly, an estimate of gradient $(\partial y/\partial\mu)$ can be obtained as

$$\frac{\partial y}{\partial \mu} \approx -S(\mu)P\frac{\partial C}{\partial \mu}y_s \tag{13}$$

if the extraneous sensor's noise source n_s is assumed to be of zero mean. The gradient estimate $(\partial y/\partial\mu)$ using NRRO components with extraneous sensor can be obtained from (13) after subtracting y_s from RRO estimator offline constructed from previous subsection and post-filtering with $(\partial C/\partial\mu)(\mu)$ with the shock transfer function model $S(\mu)P$.

Although the use of an additional sensor incurs an extra cost, the main advantage of the extraneous sensor is obvious as reinjecting measured PES e into the servo system, as suggested in the previous section, becomes redundant. The convergence time of the proposed OICA will hence be halved and, similarly to that without extraneous sensor, the gradient estimate $(\partial y/\partial\mu)$ is independent of disturbances sources d_i and d_o. The unbiased experimental gradient estimate of $(\partial \hat{y}/\partial\mu)$ obtained will be sufficiently accurate if the noise levels from both the servo system n and extraneous sensor n_s are low, as well as if length of data logged N is large due to the expectation (or averaging) operation from (5).

Similarly using these data and the previously stored NRRO data in $\boldsymbol{N}$, (5) is used to calculate the partial derivative of cost function with respect to controller parameter $(\partial J/\partial\mu)$ at current iteration i.

D. Parametric Update

With the developments derived with and without the usage of an extraneous sensor, the controller parameter vector μ is then updated with the following iterative algorithm at the end of each iteration i by

$$\begin{aligned}\mu(i+1) &= \mu(i) - \frac{\partial J}{\partial \mu}(i) \\ &= \mu(i) - \frac{2}{N-1}\sum_{k=1}^{N} y(k)\frac{\hat{\partial} y}{\partial \mu}(k)\end{aligned} \tag{14}$$

by replacing the gradient estimate of $(\partial y/\partial\mu)$ with the unbiased experimental gradient estimate of $(\hat{\partial} y/\partial\mu)$. The updating algorithm in (14) is in essence a steepest decent algorithm, i.e., the parameters are updated in the direction of steepest drop in gradient of $J(\mu)$. The proof of parametric convergence is detailed in [4] and is omitted here for brevity but without loss of generality. The convergence rate is not as rapid as that using the Gauss–Newton method, but is essential for real-time implementation to save computational cycles and power from having to evaluate matrix inverses.

IV. System Evaluation

To demonstrate the effectiveness of our proposed OICA, the control scheme without an extraneous sensor will be evaluated with simulation and experimental results, using the PC-based servo system setup on a spinstand, as reported previously in [15].

A. Spinstand Servo System

For our evaluation of the proposed OICA, the Guzik spinstand (Model S1701A)[1] is used. The existing head cartridge of the spinstand is modified to integrate a small piezoelectric actuator (of dimensions 3 mm × 3 mm with a displacement range of about 140 μin) near to the R/W head. The width of the write head element used, is about 10.5 μin and the width of the giant magnetoresistance (GMR) read element is about 8.4 μin. In this experiment, the track pitch is 9 μin as documented in [15]. A schematic diagram of the architecture of the PC-based servo system is shown in Fig. 3 and a close-up view of the head cartridge with a piezoelectric PZT (Pb-Zr-Ti) actuator is shown in Fig. 4.

The controlled plant P has four components, namely the PZT amplifier of gain twenty, the PZT actuator, the head cartridge base, and a passive suspension with the head gimbal assembly (HGA). The experimental frequency response of the PZT-actuated HGA (with passive suspension) using calibrated measured PES e (without control) is shown in Fig. 5. It can be seen from Fig. 5 that PZT-actuated HGA has the first in-plane structural resonant sway mode at 4.2 kHz.

The identified plant is discretized via zero order hold (ZOH) method and a sampling time of 65 μs is chosen according to PC-based servo system setup specifications and required computation time as reported previously in [15]. The transfer function of the identified PZT-actuated HGA's plant model in z-domain is

$$P(z) = -3.3291z^{-1}\frac{z + 0.8862}{z^2 + 0.3695z + 0.7236}. \tag{15}$$

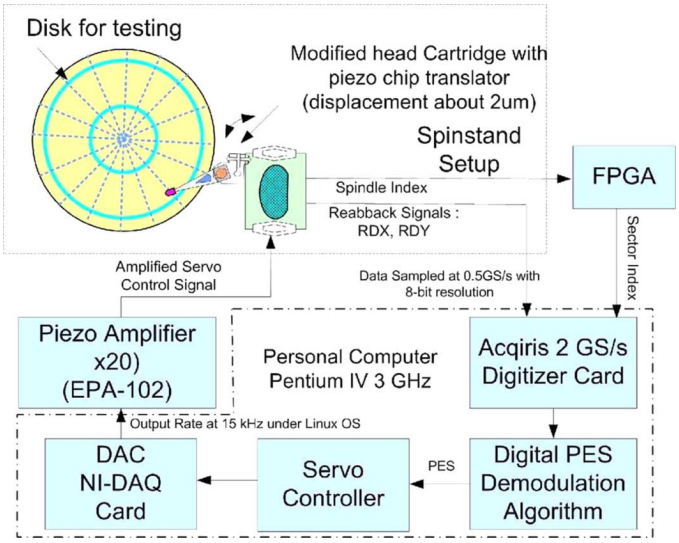

Fig. 3. Schematic diagram of the architecture of the PC-based servo system.

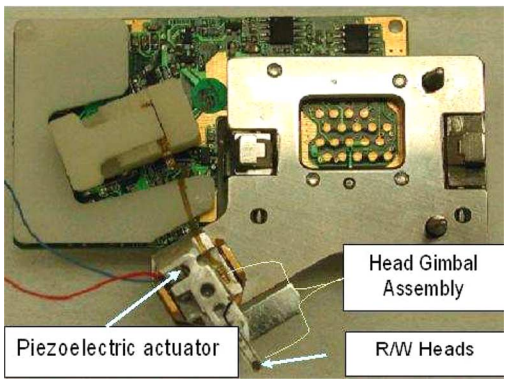

Fig. 4. Modified head cartridge with piezoelectric (PZT) actuator, HGA (with passive suspension), and R/W head.

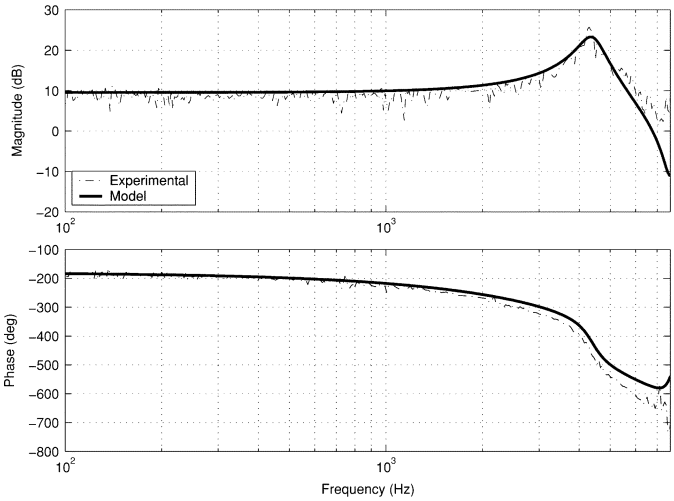

Fig. 5. Frequency response of PZT-actuated HGA (with passive suspension) measured with PES.

To demonstrate the effectiveness of the proposed OICA, a nominal feedback controller $(U(z)/E(z))$ which is in essence a first-order lag controller cascaded with an approximate plant inverse designed using the guidelines in [13]

$$\frac{U(z)}{E(z)} = -0.051079\frac{z-0.04321}{z-1}\frac{z^2+0.3695z+0.7236}{(z-0.1658)^2} \tag{16}$$

is used to ensure low sensitivity according to discrete Bode's integral theorem. Rewriting (16) into filter form

$$\begin{aligned}\frac{U(z^{-1})}{E(z^{-1})} &= \frac{U(z^{-1})}{\Xi(z^{-1})}\frac{\Xi(z^{-1})}{E(z^{-1})} \\ &= \frac{-0.05108-0.01666z^{-1}-0.03615z^{-2}+0.001597z^{-3}}{1-1.331z^{-1}+0.3589z^{-2}-0.02748z^{-3}}\end{aligned} \tag{17}$$

and augmenting the pole polynomial $(\Xi(z^{-1})/E(z^{-1}))$ to form the shaped plant to be controlled, parametric updates will be done only on the coefficients of the zero polynomial $(U(z^{-1})/\Xi(z^{-1}))$ to prevent closed-loop instability. Hence, the zero polynomial $(U(z^{-1})/\Xi(z^{-1}))$ can be expressed as an FIR filter $C(\mu)(z^{-1})$ as

$$\begin{aligned}C(\mu)(z^{-1}) &= \mu_0+\mu_1 z^{-1}+\mu_2 z^{-2}+\mu_3 z^{-3} \\ &= \boldsymbol{\mu}^T\boldsymbol{\xi}(z^{-1})\end{aligned} \tag{18}$$

and the FIR filter $C(\mu)(z^{-1})$ is parameterized by vector $\boldsymbol{\mu} = [\mu_0\,\mu_1\,\mu_2\,\mu_3]^T$ with $\boldsymbol{\xi}(z^{-1})$ as a vector of delay operators as mentioned earlier in Remark 1 of Section II. $C(\mu)(z^{-1})$ is initialized to coefficients of zero polynomial $(U(z^{-1})/E(z^{-1}))$ in (17).

To prevent controller and actuator saturation, a simple and effective anti-windup compensator $W(z)$ of the form

$$W(z) = \alpha z^{-1} \tag{19}$$

with $0 < \alpha \leq 1$ is included as seen in Fig. 2. $W(z)$ works only when the control signal is saturated. The induced oscillations during parametric adaptations during large-span seek operations are also greatly reduced.

For the PC-based servo system on spinstand, the time responses of NRRO and corresponding control signal before using the proposed OICA are shown in Fig. 6. The corresponding experimental frequency spectra of PES, RRO, and NRRO are shown in Fig. 7.

From the above figures, a 3σ NRRO of 0.7823 μin translating to 127 kTPI at 10% tolerance is observed. It should be noted that the less than exemplary responses obtained (corresponding to lower kTPI) are due to usage of an earlier generation of spindle motor.

B. Performance Evaluation

In this section, the PC-based servo system on spinstand described in the previous subsection is used to illustrate the effectiveness of the proposed OICA scheme in NRRO rejection. The OICA consists of collecting N samples of measured PES e (chosen to be at least two revolutions of the spindle speed) for constructing an online RRO estimator at each update as shown in Fig. 2. For our experiments, the spindle rotation speed

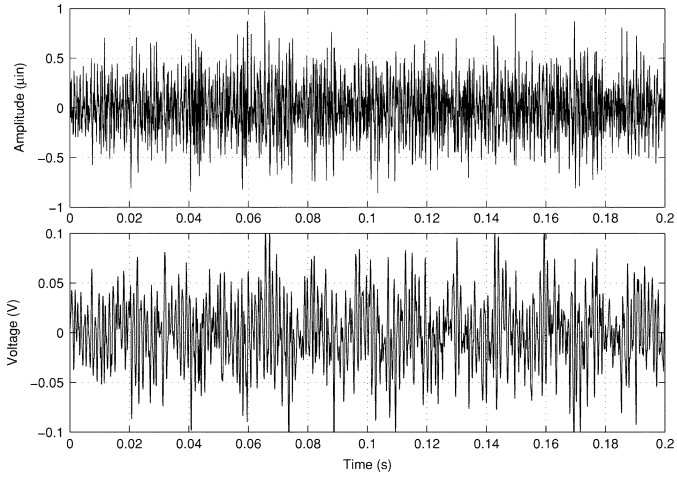

Fig. 6. Time traces before using proposed OICA. Top: NRRO. Bottom: control signal. A 3σ NRRO of 0.7823 μin translating to 127 kTPI at 10% tolerance is observed.

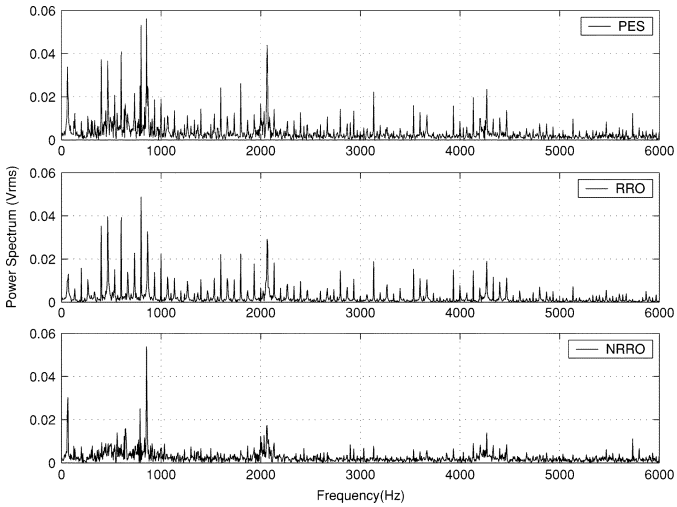

Fig. 7. Experimental measured frequency spectra before using proposed OICA. Top: PES. Middle: RRO. Bottom: NRRO.

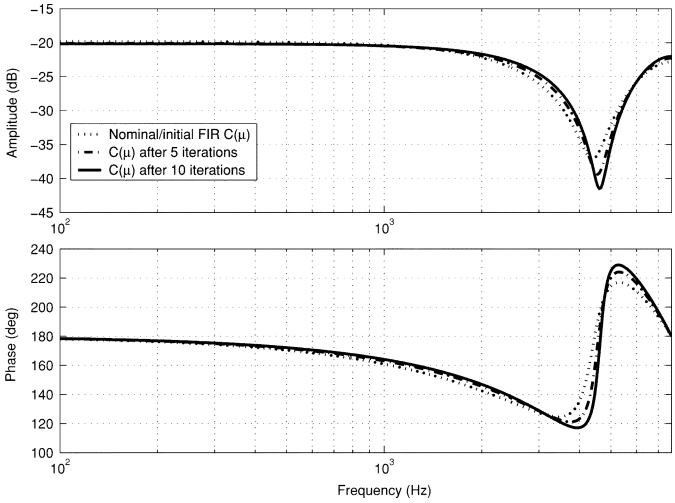

Fig. 8. Frequency responses of FIR filter $C(\mu)$. Dotted: nominal. Dashed-dot: after five iterations using proposed OICA. Solid: after ten iterations of using proposed OICA.

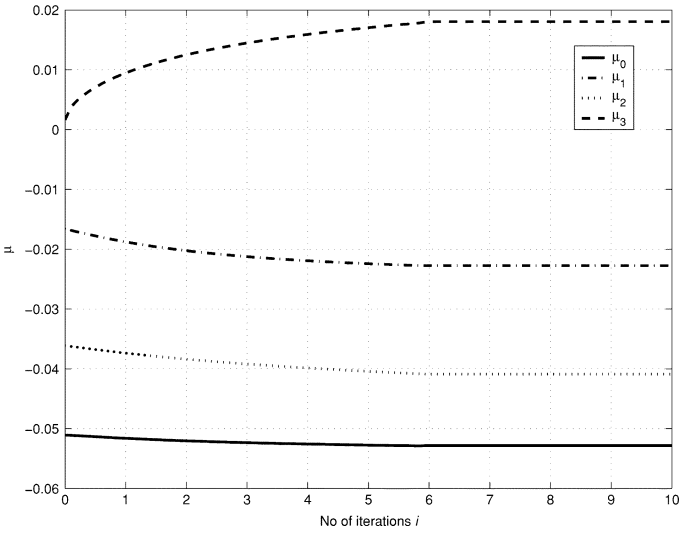

Fig. 9. Parameters μ_0 to μ_3 of FIR filter $C(\mu)$ when using proposed OICA. The parameters of FIR filter $C(\mu)$ typically converge after six iterations of using proposed OICA.

is 4000 rpm and five spindle revolutions are used. As such, $N = 1154$ and the lengths of the PES buffer $\boldsymbol{E}$, RRO buffer $\boldsymbol{R}$ and NRRO buffer $\boldsymbol{N}$ are set as N. It should be noted that the FIR filter $C(\mu)$ is not updated during this iteration (i.e., $i = 0$) for data logging.

1) FIR Filter $C(\mu)$: Using the proposed OICA, the evolution of the FIR filter $C(\mu)$ using proposed OICA after ten iterations is shown in Fig. 8. It can be seen that the zeros of the notch filter originally designed to attenuate the gain of the PZT actuator's sway mode at 4.2 kHz are shifted to 4.8 kHz with a smaller damping ratio. The effects and explanations will be investigated with experimental measured PES e later.

The parameters of the FIR filter $C(\mu), \mu_0$ to μ_3, after ten iterations of using proposed OICA are shown in Fig. 9. Although the steepest descent method parametric updating method is used, the parameters typically converge to their optimal values, i.e., $\mu = \mu^*$, after six iterations of OICA tuning.

2) Robustness Analysis: The robustness margin of the proposed OICA is investigated with simulation examples using the same set of collected PES, RRO, and NRRO data during the ten iterations of OICA as mentioned in the previous subsection. The effects of variations in natural frequencies of the actuators and different initial controller conditions are mimicked by perturbing the gain and notch frequency (initially at natural frequency of PZT actuator's in-plane sway mode of 4.2 kHz) with $\pm 10\%$ variations. The frequency responses of the perturbed, nominal, and optimal FIR filter $C(\mu^*)$ are shown in Fig. 10.

Using the proposed OICA, both the perturbed and nominal FIR filters converge to optimal FIR filter $C(\mu^*)$. However, the rate of convergence depends on the size of norm of difference between the initial controller parameter and that of optimal parameter vector μ^*. For the case of -10% shift in gain and notch frequency shown in Fig. 10, ten iterations are needed while only three iterations are required for the case of $+10\%$ shift in gain and notch frequency.

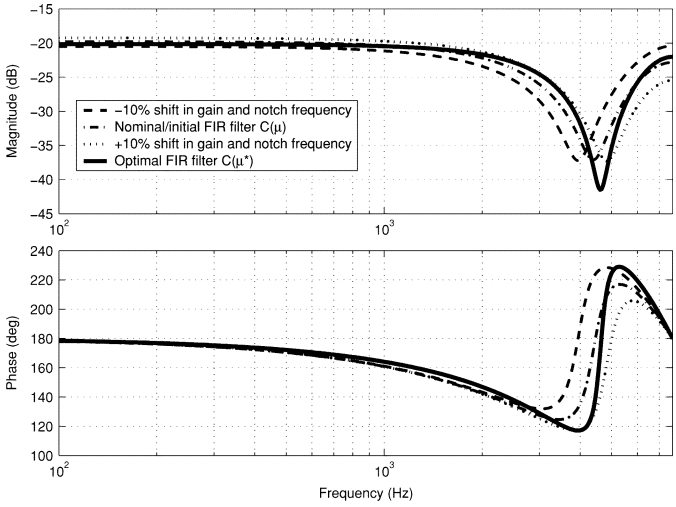

Fig. 10. Frequency responses of FIR filter $C(\mu)$ with $\pm 10\%$ shift in gain and notch frequency. Dash: -10% shift in gain and notch frequency of FIR filter $C(\mu)$. Dash-dot: nominal FIR filter $C(\mu)$. Dot: $+10\%$ shift in gain and notch frequency of FIR filter $C(\mu)$. Solid: optimal FIR filter $C(\mu^*)$.

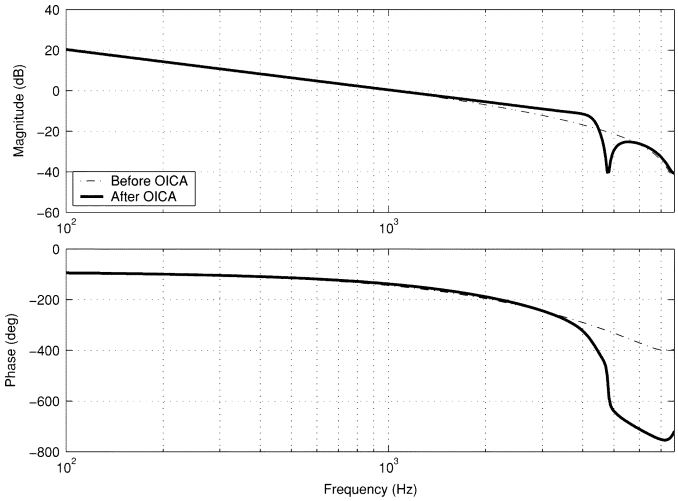

Fig. 11. Frequency responses of open loop transfer functions. Dashed-dot: before using proposed OICA. Solid: after six iterations of using proposed OICA.

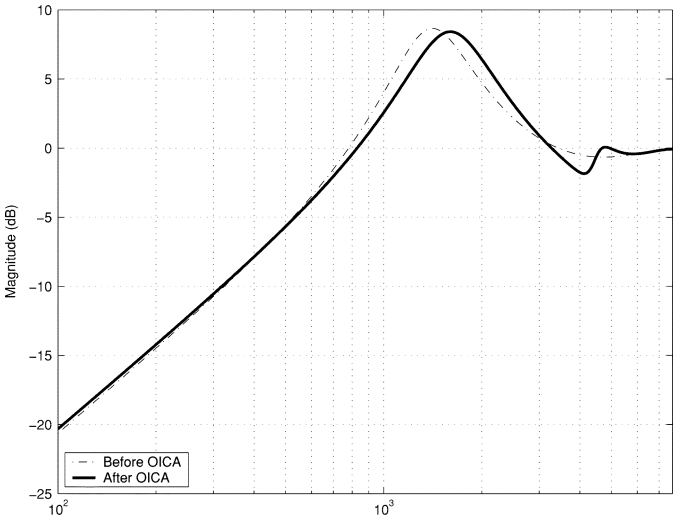

Fig. 12. Frequency responses of sensitivity transfer functions. Dashed: before using proposed OICA. Solid: after six iterations of using proposed OICA. Two sensitivity transfer function notches are created in frequency regions of 3–5 kHz and 5–7 kHz.

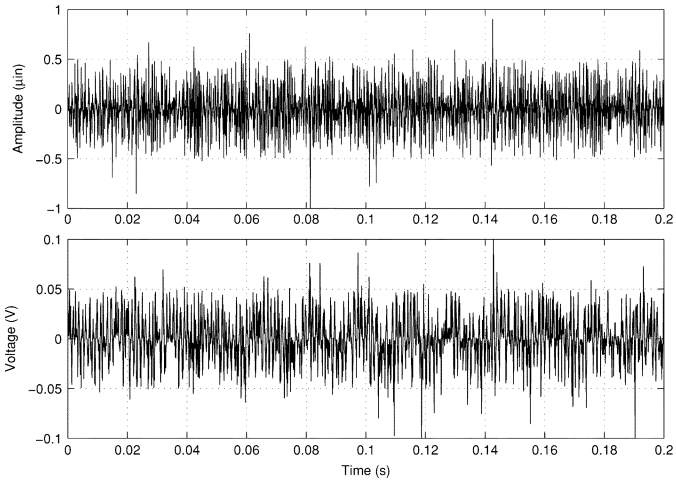

Fig. 13. Time traces after six iterations of OICA tuning. Top: NRRO. Bottom: control signal. A 3σ NRRO of 0.6101 μin translating to 164 kTPI at 10% tolerance or 22% improvement is observed.

3) Frequency Responses: The frequency responses of the open loop transfer functions using nominal controller $(U(z)/E(z))$ and that with FIR filter $C(\mu)$ using the proposed OICA algorithm for six iterations are shown in Fig. 11. With the same controller order, the proposed OICA achieves better disturbance rejection even without prior knowledge of the disturbance model, or an increase the open loop gain crossover frequency for higher bandwidth and stronger disturbance rejection.

The frequency response of the sensitivity transfer functions using nominal controller $(U(z)/E(z))$ and that of the FIR filter $C(\mu)$ using the proposed OICA algorithm for six iterations are shown in Fig. 12. The proposed OICA seeks to increase the gain at the resonant modes to create an attenuation notch in the sensitivity transfer function around the resonant mode frequency region of 3–5 kHz where the PZT actuator's in-plane sway mode is and much of the high-frequency NRRO spectrum is trapped. Another notch in sensitivity transfer function of smaller magnitude is also created at around 5–7 kHz region where much high-frequency NRRO is concentrated at as shown earlier in Fig. 7.

4) Time Responses: The time responses of the NRRO and control signal after six iterations of using proposed OICA are shown in Fig. 13. It can be seen from Figs. 6 and 13 that much of the variance of NRRO is reduced after six iterations of using proposed OICA. The 3σ NRRO is reduced to 0.6101 μin, translating to 164 kTPI at 10% tolerance or a 22% reduction in 3σ NRRO over the nominal controller when computed. The histograms of NRRO before and after OICA tuning are shown in Fig. 14.

The power spectra of the experimental NRRO before and after six iterations of using the proposed OICA are shown in Fig. 15. As can be seen from the NRRO spectrum before using the proposed OICA in Fig. 7, much NRRO is trapped in the frequency

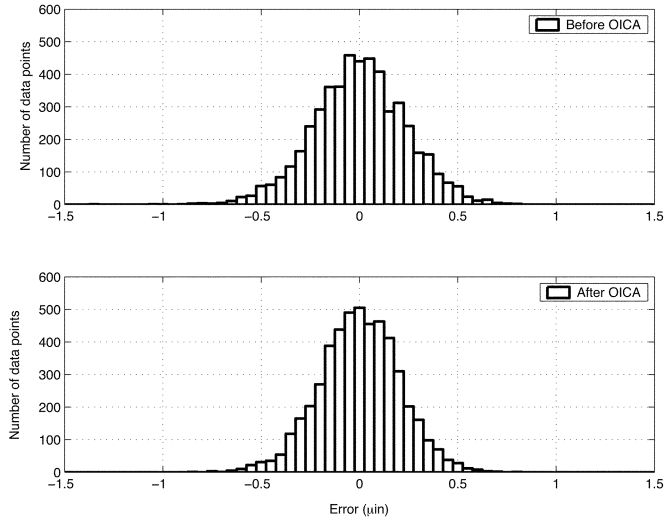

Fig. 14. Histograms of NRRO spectrum. Top: before using proposed OICA tuning. Bottom: after six iterations of using proposed OICA tuning.

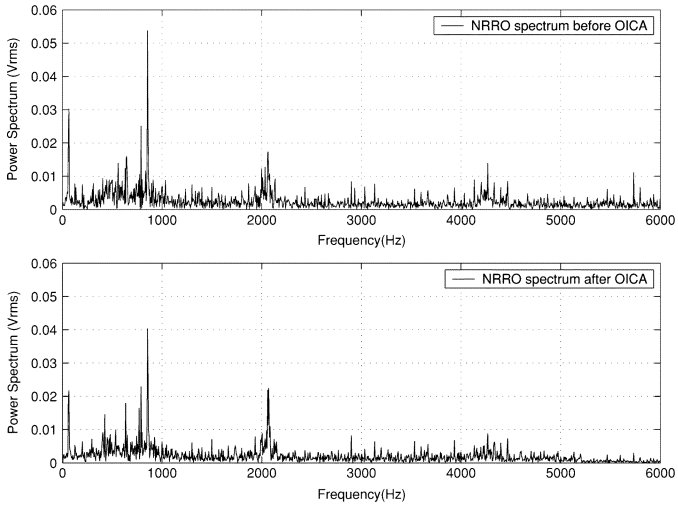

Fig. 15. Experimental NRRO spectrum. Top: before using proposed OICA. Bottom: after six iterations of using proposed OICA. Much reduction of baseline NRRO and stronger NRRO rejection at frequency regions of 3–5 kHz and 5–7 kHz are observed.

region 3–5 kHz corresponding to the PZT actuator's sway mode at resonant frequency of 4.2 kHz and also in the high-frequency region of about 5–7 kHz. With the attenuation notches in the sensitivity transfer function created at these frequency regions, the improvement in NRRO spectrum after OICA shows much amplitude reduction as shown in Fig. 15. The baseline NRRO at most frequencies is also effectively suppressed by the controller after six iterations of using the proposed OICA.

V. Conclusion

In this paper, an online iterative control algorithm (OICA) is proposed to minimize the square of $\mathcal{H}_2$-norm of T_{yw}, hence avoiding any ill-conditioned numerical issues commonly encountered when solving AREs and LMIs in robust and optimal controller synthesis for HDDs. The TMR budget is optimized for achieving higher recording densities via stronger NRRO rejection in future HDDs. Experimental results using the proposed OICA on a third order FIR in a PC-based servo system on spinstand show an improvement of 22% in 3σ NRRO and much baseline NRRO rejection without increase in servo bandwidth for stronger disturbance rejection. Our future works include implementing the proposed OICA with SSA in STW processes for ultrahigh-track density demonstrations on a spinstand servo system.

References

[1] *Guzik Company Website*, Spin Stand Products Information [Online]. Available: http://www.guzik.com

[2] A. Al-Mamun, T. H. Lee, G. Guo, W. E. Wong, and W. Ye, "Measurement of position offset in hard disk drive using dual frequency servo bursts," *IEEE Trans. Instrum. Meas.*, vol. 52, no. 6, pp. 1870–1880, Dec. 2003.

[3] Y. Chen and K. L. Moore, "Iterative learning control with iteration-domain adaptive feedforward compensation," in *Proc. 42nd IEEE CDC*, Maui, HI, Dec. 9–12, 2003, pp. 4416–4421, ThP09-3.

[4] J. E. Dennis and R. B. Schnabel, *Numerical Methods for Unconstrained Optimization and Nonlinear Equations*. Philadelphia, PA: SIAM, 1996.

[5] T. B. Goh, Z. Li, B. M. Chen, T. H. Lee, and T. Huang, "Design and implementation of a hard disk drive servo system using robust and perfect tracking approach," *IEEE Trans. Control Syst. Technol.*, vol. 9, no. 2, pp. 221–233, Mar. 2001.

[6] H. Halmarsson, M. Gevers, S. Gunnarsson, and O. Lequin, "Iterative feedback tuning: Theory and applications," *IEEE Control Syst. Mag.*, vol. 18, no. 4, pp. 26–41, Aug. 1998.

[7] Q. Hao, R. Chen, G. Guo, S. Chen, and T. S. Low, "A gradient-based track-following controller optimization for hard disk drive," *IEEE Trans. Ind. Electron.*, vol. 50, no. 1, pp. 108–115, Feb. 2003.

[8] G. Herrmann and G. Guo, "HDD dual-stage servo-controller design using a μ-analysis tool," *Control Eng. Practice*, vol. 12, no. 3, pp. 241–251, Mar. 2004.

[9] Q. W. Jia, F. C. Cai, and Z. F. Wang, "Repeatable runout disturbance compensation with a new data collection method for hard disk drive," *IEEE Trans. Magn.*, vol. 41, no. 2, pp. 791–796, Feb. 2005.

[10] H. S. Lee, "Controller optimization for minimum position error signals of hard disk drives," *IEEE Trans. Ind. Electron.*, vol. 48, no. 5, pp. 945–950, Oct. 2001.

[11] Z. Li, G. Guo, B. M. Chen, and T. H. Lee, "Optimal track-following design for the highest tracks per inch in hard disk drives," in *J. Inf. Stor. Process. Syst.*, Apr. 2001, vol. 3, no. 1–2, pp. 27–41.

[12] C. K. Pang, G. Guo, B. M. Chen, and T. H. Lee, "Self-sensing actuation for nanopositioning and active-mode damping in dual-stage HDDs," *IEEE/ASME Trans. Mechatronics*, vol. 11, no. 3, pp. 328–338, Jun. 2006.

[13] C. K. Pang, D. Wu, G. Guo, T. C. Chong, and Y. Wang, "Suppressing sensitivity hump in HDD dual-stage servo systems," *Microsyst. Technol.*, vol. 11, no. 8–10, pp. 653–662, Aug. 2005.

[14] S. W. Park, J. Jeong, H. S. Yang, Y. P. Park, and N. C. Park, "Repetitive controller design for minimum track misregistration in hard disk drives," *IEEE Trans. Magn.*, vol. 41, no. 9, pp. 2522–2528, Sep. 2005.

[15] W. E. Wong, L. Feng, Z. He, J. Liu, C. M. Kan, and G. Guo, "PC-based position error signal generation and servo system for a spinstand," *IEEE Trans. Magn.*, vol. 41, no. 11, pp. 4315–4322, Nov. 2005.

[16] D. Wu, G. Guo, and T. C. Chong, "Midfrequency disturbance suppression via micro-actuator in dual-stage HDDs," *IEEE Trans. Magn.*, vol. 38, no. 5, pp. 2189–2191, Sep. 2002.

[17] J. X. Xu and Y. Tan, *Linear and Nonlinear Iterative Learning Control*, ser. Lecture Notes in Control and Information Sciences, 291. New York: Springer-Verlag, 2003.

[18] H. Ye, V. Sng, C. Du, J. Zhang, and G. Guo, "Radial error propagation issues in self-servo track writing technology," *IEEE Trans. Magn.*, vol. 38, no. 5, pp. 2180–2812, Sep. 2002.

[19] E. Trulsson and L. Ljung, "Adaptive control based on explicit criterion minimization," *Automatica*, vol. 21, no. 4, pp. 385–399, Jul. 1985.

Manuscript received February 10, 2006; revised December 20, 2006. Corresponding author: C. K. Pang (e-mail: ckpang@nus.edu.sg.).

Chee Khiang Pang (S'04–M'07) was born in Singapore in 1976. He received the B.Eng. (Hons.) and M.Eng. degrees in 2001 and 2003, respectively, and is working toward the Ph.D. degree, all in electrical and computer engineering, from National University of Singapore (NUS), Singapore.

From February to June 2003, he was a Visiting Scholar in the School of Information Technology and Electrical Engineering, University of Queensland, Brisbane, QLD, Australia. Since April 2006, he has been with Storage Technology Research Center, Central Research Laboratory, Hitachi Ltd., Kanagawa, Japan. His current research interests include vibration analysis and servo control in sampled-data mechatronics, multisensing and active control in hard disk drives, and the self servo-track writing process.

Wai Ee Wong (M'06) received the B.Eng. degree in electrical and computer engineering and the M.Eng. degree from the National University of Singapore (NUS) in 2001 and 2003, respectively.

Currently, she is a Research Engineer at A*Star Data Storage Institute, Singapore. Her research interests include PES generation methods in data storage channels, servo track writing, and patterning for future storage devices.

Guoxiao Guo (S'95–M'96–SM'05) received the B.Eng. and M.Eng. degrees from the Department of Automation, Tsinghua University, Beijing, China, in 1989 and 1994, respectively, and the Ph.D. degree from the School of Electrical and Electronic Engineering, Nanyang Technological University, Singapore, in 1997.

He joined the A*STAR Data Storage Institute in 1995 as Research Engineer and later as the Manager of the Mechatronics and Recording Channel Division. He is also an Adjunct Fellow at the National University of Singapore, and Adjunct Associate Professor at the Nanyang Technological University. His research focuses on vibration analysis, sensing and control, mechatronics and MEMs, nonlinear and robust control for achieving nano-positioning systems in ultrahigh-density magnetic recording. He has published over 50 refereed journal papers and six patents on these topics.

Dr. Guo was the publication chairman/co-chair for the Asia-Pacific Magnetic Recording Conferences 2000 held in Tokyo, Japan, 2002 in Singapore, and 2004 in Seoul, Korea, all focused on the mechanical and manufacturing aspects of magnetic recording systems. Since June 2005, he has been Associate Editor of the IEEE TRANSACTIONS ON CONTROL SYSTEMS TECHNOLOGY.

Ben M. Chen (S'89–M'92–SM'00–F'07) was born in Fuqing, Fujian, China, in 1963. He received the B.S. degree in computer science and mathematics from Xiamen University, Xiamen, China, in 1983, the M.S. degree in electrical engineering from Gonzaga University, Spokane, WA, in 1988, and the Ph.D. degree in electrical and computer engineering from Washington State University, Pullman, in 1991.

From 1992 to 1993, he was an Assistant Professor in the Electrical Engineering Department, State University of New York at Stony Brook. Since 1993, he has been with the Department of Electrical and Computer Engineering, National University of Singapore, where he is currently a Professor. His current research interests are in robust control, systems theory, and control applications. He is the author/coauthor of seven research monographs including *Hard Disk Drive Servo Systems* (Springer, 1st ed. 2002, 2nd ed. 2006); *Linear Systems Theory: A Structural Decomposition Approach* (Birkhauser, 2004); and *Robust and H∞ Control* (Springer, 2000). He was an Associate Editor for *Asian Journal of Control*, and is currently serving as an Associate Editor of *Automatica, Control and Intelligent Systems,* and *Systems and Control Letters*.

Dr. Chen was an Associate Editor for the IEEE TRANSACTIONS ON AUTOMATIC CONTROL.

Tong Heng Lee (M'90) received the B.A. degree with first class honors in the Engineering Tripos from Cambridge University, Cambridge, U.K., in 1980 and the Ph.D. degree from Yale University, New Haven, CT, in 1987.

He is a Professor in the Department of Electrical and Computer Engineering at the National University of Singapore. His research interests are in the areas of adaptive systems, knowledge-based control, intelligent mechatronics and computational intelligence. He has co-authored three research monographs, and holds four patents (two of which are in the technology area of adaptive systems, and the other two are in the area of intelligent mechatronics). He currently holds Associate Editor appointments in *Automatica*; *Control Engineering Practice* (an IFAC journal); the *International Journal of Systems Science* (Taylor and Francis, London); and *Mechatronics* journal (Oxford, Pergamon Press).

Dr. Lee was a recipient of the Cambridge University Charles Baker Prize in Engineering. He is an Associate Editor of IEEE TRANSACTIONS ON SYSTEMS, MAN, AND CYBERNETICS